PHASE I OPERATIONS

K500 CYCLOTRON OPERATING EXPERIENCE

P. Miller, D. Poe, H. Thulin

Reliability of operation of the K500 has improved over the past year. Statistics of time use from 1 January 1986 to 31 December 1986 are given in Table I. Two items stand out: 1) There was a significant amount of shutdown time associated with the installation of the room temperature ECR injection line (January through March) and of the permanent ECR power supply and controls as well as the water cooled resonators (December). 2) The reliability of operation (defined as the percentage of breakdown time as a fraction of total scheduled operating time equals (Research + Development + Overhead)/(Total - Off - Maintenance)), is up substantially, 75% compared to 58% last year. Overhead is also slightly higher, probably reflecting the learning curve associated with changing ECR beams and tuning the ECR injection line.

Table I--Time Distribution (1986)

Use category	Hours	Fraction of operating period
Operation		
Research	2256	35.0 %
Development	671	10.4 %
Overhead[a]	1219	18.9 %
	4146	64.3 %
Maintenance	884	13.7 %
Breakdowns	1418	22.0 %
Total	6448	100.0 %
Off (shutdown periods)	2313 h	

a. "Overhead" represents time used for tuning of the cyclotron, ion source and beam lines, and deflector conditioning, i.e. operations other than research and development.

Operation of the K500 with the ECR source began in March 1986 after the injection beamline was installed; there was no operation using the PIG source after Dec. 1985.

The beams provided by the cyclotron and the total time external beam was available for each are listed in Table II. Twenty four PAC-authorized experiments were completed in 1986; in addition there were 14 beam runs for development of equipment and techniques.

ECR-K500 Injection Line

The ion charge state is selected by a 90° bending magnet. An identical magnet is required to bend the beam upward toward the aperture below the spiral electrostatic inflector inside the cyclotron. The line also contains a 23° horizontal bending magnet, 5 x-y steering magnets and 5 solenoids. Beam diagnostics include 5 Faraday cups for measuring beam current, one 2-jaw and six 4-jaw collimators with current readout from each jaw fed to a computer for simultaneous graphical display. A two-grid rf buncher (only one grid is presently used due to inherent non-isochronism of the injection path inside the magnet pole) increases the average beam current accepted for acceleration by the cyclotron by a factor between 2 and 5. Transmission efficiency was 2 to 5% (from source analyzer output to cyclotron external beam stop) during the first few months of operation. Transmission has recently decreased to less than 1% primarily due to losses in the latter part of the injection line. Causes for these losses are under investigation.

Dee Stem Cooling

The dee stem cooling improvements reported last year did not remain effective; however, a new approach appears to have finally solved the problem. Water cooling lines were installed on the corona rings and were connected using polyethylene tubes inside the resonator. These tubes are exposed to rf fields (peak voltage 60 kV at 19 MHz). No degradation due to sparking

or rf heating effects is observed. The surface temperature of the copper corona rings has been lowered substantially (100°F or more at 80 kV) and the rate of oxidation of the copper has been reduced to the point where it is not noticeable. We have completed experiments running 85 kV peak on the dees, which was not possible before the water cooling was added.

Second Harmonic Acceleration

The K500 has successfully accelerated several beams with the rf running at 2X the ion frequency using the central region geometry designed for the first harmonic, in agreement with orbit calculations.

Table II--Beams Provided in 1986

Ion	E/A [MeV/u]	% Time	Hours of external beam
$^{2}H^{1+}$	53	2.1	57.8
$^{4}He^{1+}$	25	3.7	100.3
$^{4}He^{3+}$	54	2.9	79.5
$^{7}Li^{1+}$	10	1.7	44.8
$^{7}Li^{2+}$	25	2.0	53.0
	30	1.3	34.5
$^{12}C^{3+}$	15	0.3	8.3
$^{12}C^{4+}$	25	1.5	40.5
	35	4.0	109.0
$^{12}C^{5+}$	40	2.3	62.0
	50	1.2	32.3
$^{14}N^{3+}$	10	0.4	9.5
$^{14}N^{4+}$	20	2.7	74.0
	30	0.1	3.5
$^{14}N^{5+}$	30	1.9	51.3
	35	27.4	739.5
$^{14}N^{6+}$	40	7.9	212.3
	45	0.4	9.8
	50	1.0	26.0
$^{16}O^{3+}$	10	0.1	4.0
$^{16}O^{5+}$	20	0.4	9.8
$^{16}O^{6+}$	30	2.4	65.7
$^{16}O^{7+}$	40	1.8	48.0
$^{16}O^{8+}$	54	0.5	12.5
$^{18}O^{5+}$	30	1.9	50.0
$^{18}O^{6+}$	35	0.5	13.0
$^{18}O^{7+}$	35	1.9	50.0
$^{20}Ne^{6+}$	25	0.5	13.3
$^{20}Ne^{7+}$	30	4.6	123.5
$^{22}Ne^{4}$	10	3.9	105.8
$^{22}Ne^{6+}$	25	0.3	7.5
$^{22}Ne^{7+}$	35	7.9	212.3
$^{36}Ar^{11+}$	35	1.1	31.0
$^{40}Ar^{7+}$	12	0.2	6.5
$^{40}Ar^{8+}$	15	0.8	20.8
$^{40}Ar^{11+}$	25	0.1	4.0
	30	1.5	40.5
	32	1.3	34.5
$^{86}Kr^{17+}$	19	2.4	64.7
$^{86}Kr^{19+}$	20	1.3	33.8
	Total	100.0	2698.5

K500 VACUUM STUDIES

M.L. Mallory

The K500 vacuum system and previous vacuum calculations have been reported in earlier annual reports.[1,2] These calculations indicated that vacuum values of 1 x 10^{-7} Torr would be necessary to accelerate the very heavy ions to full energy with 90% tranmission. Up to the present time, only heavy ions with masses up to 86 have been accelerated in the K500 cyclotron.

With the operation of the ECR ion source, high charge state heavier ions are now available. The vacuum requirements for these charge states were calculated, using a computer code which has been updated to include the latest charge pickup and stripping cross sections[3]. The results of the calculations are summarized in fig. 1 and indicate that the losses for the high charge ions are primarily due to charge pickup processes at small radii in the cyclotron. For a vacuum value of 3 x 10^{-6} Torr, a tranmission percentage less than 10% is to be expected for U^{25+} ions. For ions lighter than mass 40 the losses are expected to be very low and this agrees with our experience. We have recently tested a krypton beam and its attenuation as a function of radius in the K500 cyclotron is shown in fig. 2. A small loss between 4 and 6 inches was detected. The losses detected at a radius of less than 4 inches are masked by rf pickup noise on the probe. The krypton beam loss observed tends to confirm the vacuum calculation. They predict a vacuum requirement of ~1 x 10^{-7} Torr for greater than 90% tranmission for U ions (agreeing with earlier results).

The present cyclotron pressure has been as low as 3 x 10^{-6} Torr. There are known air leaks and water leaks. Some of these leaks are scheduled to be fixed in early March, 1987. The RGA indicates that air is presently the dominant residual gas. Fixing the above leaks should allow the vacuum to approach its base value, which is expected to be dominated by the outgassing of the cyclotron interior. Previous experience with other large systems indicates that the vacuum required is ~1 x 10^{-6} Torr, with water as the dominate gas load. To obtain lower vacuum in a reasonable time, one then needs to bake out the vacuum system. This is not possible for the K500 cyclotron.

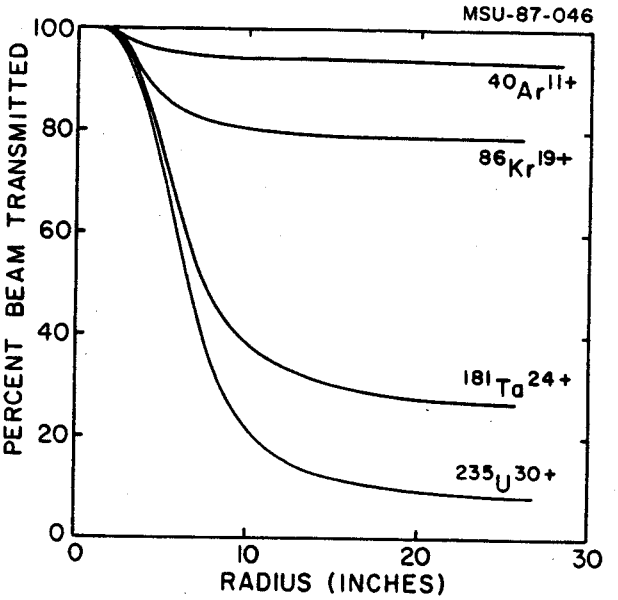

Fig. 1. The vacuum attenuation for various heavy ion species have been calculated for a pressure of 3 x 10^{-6} Torr. Large losses are predicted for the very heavy ion beams

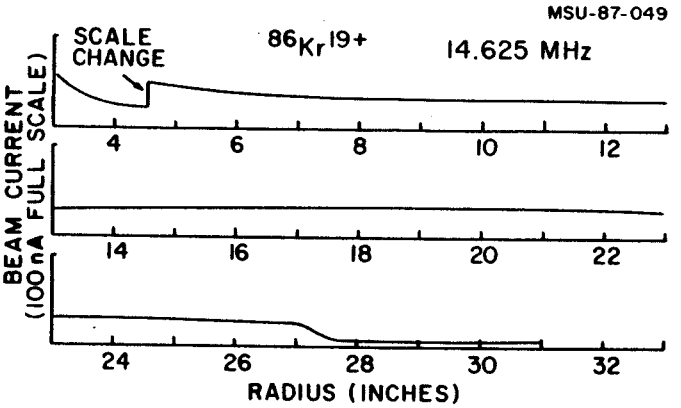

Fig. 2. An experimental krypton beam has been tested in the K500 cyclotron and its attenuation at small radii tends to confirm the vacuum calculations.

Fortunately, a new technological approach[4] for outgassing vacuum surfaces has recently appeared and has been tested in an extraction beam line at Brookhaven[5]. This approach is to illuminate the surfaces with UV light. Using this method could be a possible solution to the K500 ultimate vacuum base problem. In addition, the UV outgassing could speed up the pump down time for the K500 cyclotron to attain excellent vacuum conditions. For example, if we assume that the K500 acceleration chamber will be opened to air once per month and that 2 days are required to attain an excellent vacuum, then UV radiation will potentially provide an additional 24 days of very heavy ion operation per year. It therefore seems very desirable to study UV upgrading of the K500 vacuum system.

References

1. NSCL Annual Report (1985) 139.
2. NSCL Annual Report (1978-79) 132.
3. A.S. Schlachter, Tenth International Conference on Cyclotron and Their Applications (1984)563.
4. Danielson Associates Inc.
5. H.C. Hseuh, J.E. Tuozzolo, to be published (1987 Particle Accelerator Conf.).

ECR INJECTION LINE VACUUM REQUIREMENTS

M.L. Mallory

The K500 cyclotron now uses an ECR ion source. This ion source is located approximately 5 m from the cyclotron. The K800 is also planned to have an ECR source located approximately 10 m from the cyclotron. The computer code used for calculating the K500 vacuum was modified to calculate the vacuum requirements of the injection line. Various ion species were studied and the vacuum was most sensitive to high charge state uranium ions. Figure 1 shows the vacuum attenuation for $^{181}Ta^{25+}$. Over 90% of the beam is expected to be transmitted for a vacuum better than 1×10^{-5} Torr. The largest cross section term for charge state change is charge pickup. The vacuum requirement is easily met by standard vacuum techniques and no losses due to vacuum have been detected in the K500 injection line.

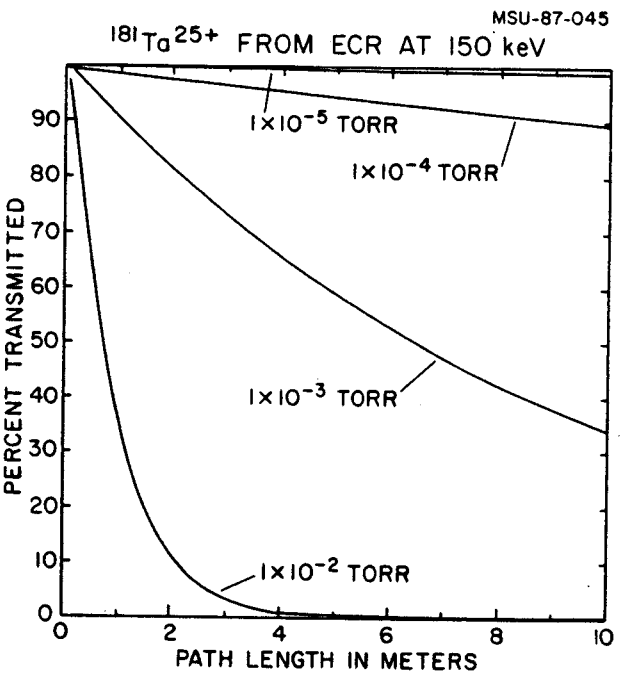

Fig. 1. The vacuum attenuation for various pressure values is calculated as a function of distance from the ECR ion source. Standard vacuum technique should easily meet these requirements.

References

1. NSCL Annual Report (1978-79) 132.

OPERATION OF LIQUID HELIUM LEVEL SENSORS AT ELEVATED PRESSURES

A.F. Zeller, H. Laumer and J.A. Nolen

The normal operational pressure of the 2500 l liquid helium (LHe) dewar is between 8 and 11 psig, corresponding to liquid temperature of 4.7 to 4.86° K. In this pressure range, the standard American Magnetics Inc. (AMI) level detector, which is based on the Efferson design[1], "sticks". The detector faithfully follows the surface when the level is falling, but does not indicate a rising level. These Efferson type detectors are a thin superconducting wire with a short bifilar wound heater. They utilize the difference in heat transfer between the liquid and gas phases to maintain a resistive zone above the liquid and remain superconducting below the surface. The level is indicated by the voltage drop across the wire. At higher pressures, and hence, temperatures, the difference in heat transfer decreases until at 18.3 psig (5.20°K) the critical point is reached (the density of the liquid and gas are equal). Thus at some pressures between 0 and 18.3 psig the resistive heating of the normal zone will be more than can be removed by the reduced heat transfer, and the resistive zone will be driven below the meniscus. At dewar pressures of 8-11 psig, the resistive zone is about in equilibrium with the surface, so it reads properly when the level is decreasing. However, a rising level does not produce enough additional cooling to cause the resistive zone to shrink, so the meter "sticks" at the lowest level.

Turning the existing current off and back on to read the true level is possible, but this effect can be eliminated by changing the heater current. Tests were done in the 500 l dewar using a standard AMI 18" sensor. The sensor was inserted to about one half its length into the liquid. The voltage drop was then measured as a function of heater current. The current was increased until the dramatic rise in voltage signaled that the wire was completely normal, then the current was decreased slowly to zero. During the decreasing current phase, the normal zone would suddenly retreat to the interface, but at a current below where it had run away on the increasing ramp. The operating range is then defined by the overlapping section of the two curves. Measured curves for three pressures are shown in fig. 1. Starting at the bottom the pressures are 14.1, 14.5 and 15 psig. The curve for 15 psig, has no operating range.

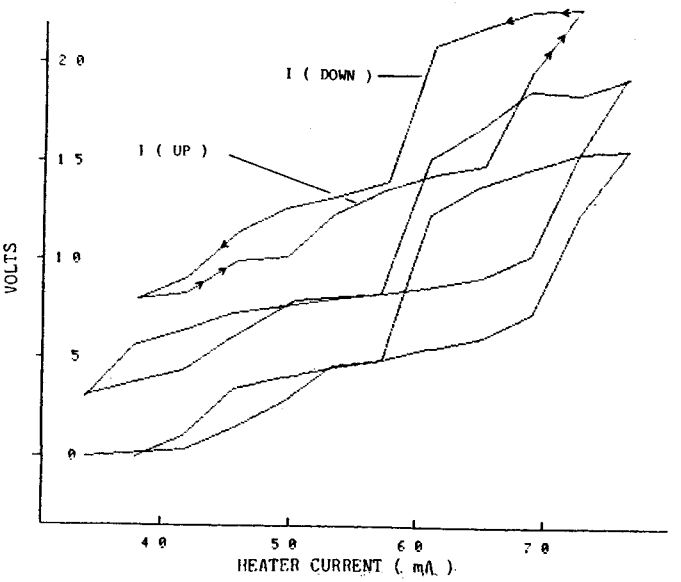

Fig. 1. Voltage drops for upward and downward ranges of the heater current for 14.1 (bottom), 14.5 and 15.0 (top) psig. 15.0 psig is near the critical point.

Curves tend to have longer operating range as the pressure is decreased, as shown in fig. 2. The line represents a reasonable operating point as a function of pressure. It would appear that a constant current of approximately 58 ma would suffice for all pressures, but operation at such a low current at low pressure would greatly reduce the response time, so currents should be

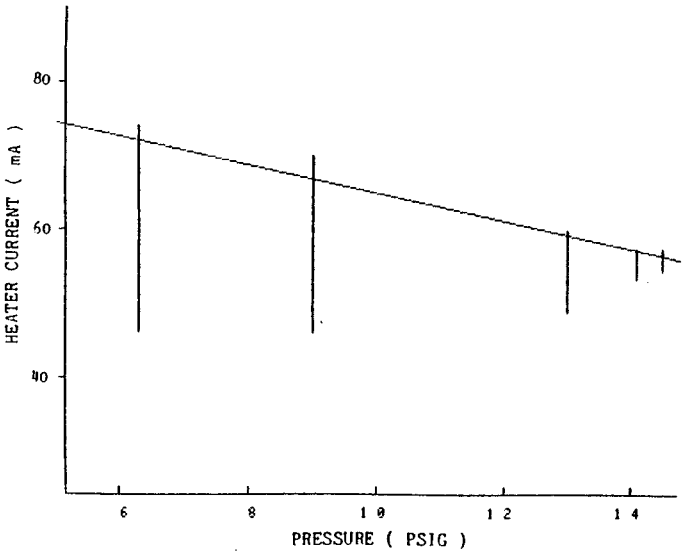

Fig. 2. Operating ranges as a function of pressure. The line represents an appropriate operating range for each pressure which insures a fast response, although the most efficient point is not very sensitive to small pressure changes.

kept at the upper end of the operating range. Operating at 58 mA at a pressure of 14.3 psig produced a linear response for the full 18" active length of the sensor, both for rising and falling levels.

In initial tests in the 500 l dewar, the pressure was changed by regulating the return gas flow. It was found that a relatively sharp temperature gradient is maintained in the dewar even at pressures above the critical point. The level sensor may as a result still indicate a level. This effect is, of course, not observed if the fluid in the dewar is disturbed, such as during filling.

In October, the standard AMI heater power supply output of 72 mA was reduced to 65mA. Since then the sticking of the level has not occurred, and faithful readings are obtained.

References

1. K.R. Efferson, Adv. Cryo. Eng. 15, 124(1969).

EXTRACTION OF ^{6}He BEAM FROM THE K500 CYCLOTRON

M.L. Mallory, R. Blue, D. Mikolas, F. Marti, W. McHarris, P. Miller, J. Nolen, R. Ronningen, W.T. Chou, and W. Olivier

In last years annual report[1], the possibility of producing radioactive ion beams from the K500 cyclotron was discussed. Since then, radioactive ion beams have been extracted from the K500 cyclotron in two experiments designed to produce ^{6}He. The first experiment used a $^{12}C^{4+}$ beam incident on a graphite target at the radius of the last orbit before extraction. The analogue beam $^{6}He^{2+}$ was detected with a particle detector located in the external beam line. A second stripper, located in the extraction channel, was instrumental in reducing the primary beam intensity to less than one particle per second and this allowed the successful detection of the radioactive analogue beams.

The second experiment used an $^{18}O^{6+}$ primary beam with the radioactive fragments being transmitted outside the vacuum beamline through a window foil to a particle detector. The energy spectrum of the detected particles is shown in Fig. 1. The low energy broad peak is due to $^{3}H^{1+}$ ions, which are not stopped in the detector. The $^{6}He^{2+}$ ions were detected at a maximum rate of 200 particle per second for a primary beam intensity of 1.6 eμA of $^{18}O^{6+}$ at the production foil target. A third and fourth peak were detected and are tentatively identified as $^{9}Li^{3+}$ and $^{12}Be^{4+}$. To help identify these ions, we recorded spectra with different thickness of aluminum inserted in front of the detector. These data are shown in Fig. 2. The emittance and energy spread of the radioactive beam was not measured but is thought to be comparable to the normally extracted cyclotron beam.

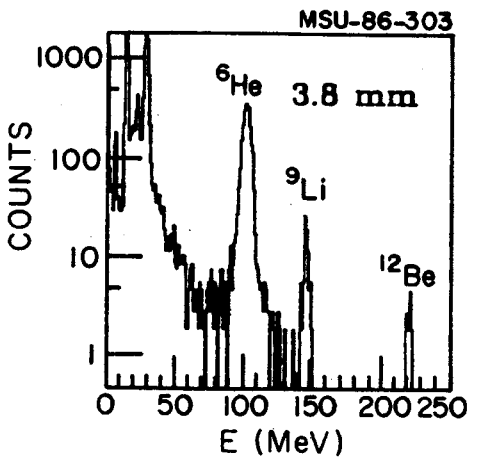

Fig. 1. The energy spectrum of radioactive fragments obtained from an $^{16}O^{6+}$ beam with a detector external to the vacuum beamline.

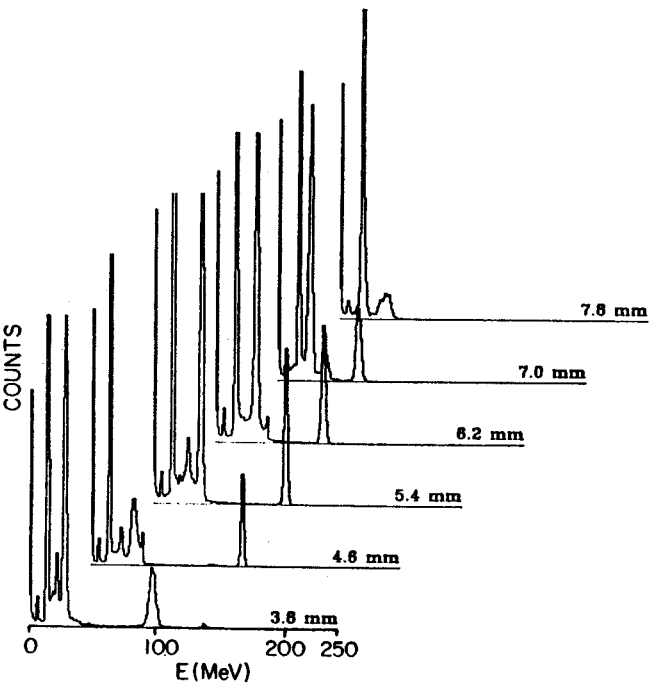

Fig. 2. The energy spectra obtained with various thicknesses of aluminum in front of the detector.

We have since realized that placing the primary beam target on the last accelerated turn removes the resonance constraint, thereby increasing the number of possible radioactive beams. Since it is not necessary for the primary and secondary beams to have the same charge to mass ratio, one may select primary beam that allows better matching of the expected

fragment cross section to the cyclotron acceptance phase space. This cross section is sharply peaked for the high energy per nucleon beams, which will be produced in the K800 cyclotron. Experiments to optimize the radioactive beam production of ^{6}He are planned for the K800.

References

1. NSCL Annual Report (1985) 187.

WATER COOLING OF THE K500 RF CORONA RINGS

M.L. Mallory, J. Kuchar, P. Miller, D. Poe, and J. Ottarson

A thermal problem with overheating of the rf corona rings was detected in the early operational stages of the K500 cyclotron. Figure 1 is a schematic drawing showing the rf stem, where it makes the transition from air to vacuum. The corona ring mounts on the air side of the vacuum insulator and its function is to provide a smooth electric field transition at the insulator. It was realized that the rf surface currents on the corona ring, coupled with the fact that the prime thermal conduction path to cooling water was through a stainless steel plate, could lead to overheating. The

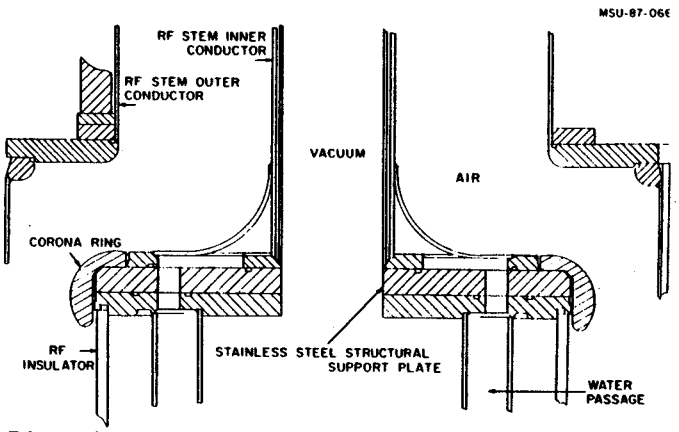

Fig. 1. A cross section drawing of the rf corona ring. The corona ring provides a smooth electric field transition at the vacuum insulator. The heat generated on the corona ring surface was initially designed to conduct through the stainless steel plate to the water cooled rf stem. The low conductivity of stainless steel allowed the corona rings to become very hot, thereby sparking and limiting the rf voltage.

stainless steel plate is a structural piece of the rf stem and provides the necessary strength needed because of the compressive forces on the insulator. It could not be easily replaced by a high conductivity material.

In several previous Annual Reports[1,2], efforts to try to bridge the stainless steel plate with high conductivity material to the water cooled surface have been reported. These efforts did not seem to solve this problem entirely. Figure 2 is a picture of a blackened corona ring. The blackening occurred when the temperature of the corona ring became excessive and at this stage the corona ring would not allow high voltage operation of the rf system. The bridged cooling of the corona ring seem to fail catastrophically and a thermal expansion model that predicted a runaway situation seems to explain many of the observations. The

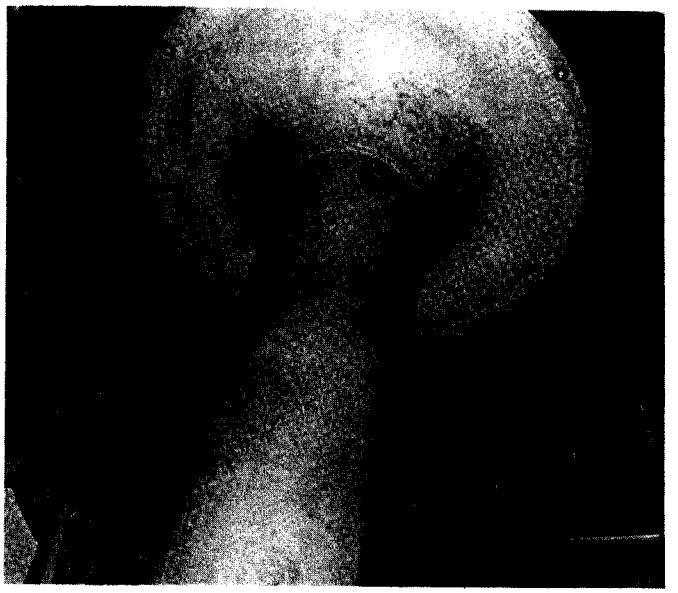

Fig. 2. A photograph of an overheated corona ring. The temperature became so hot, that a black oxide coating appeared on the outer surface of the ring.

temporary operational solution to this problem was to restrict the maximum dee voltage. Figure 3 is the operating diagram of the K500 cyclotron and the consequence of restricting the dee voltage to 70KV was the elimination of the high energy per nucleon heavy ions.

A proposal to provide direct water cooling to the corona rings similar to the way the rf amplifier components are cooled was implemented successfully. The low conductivity water is supplied via polyethylene tubes which must

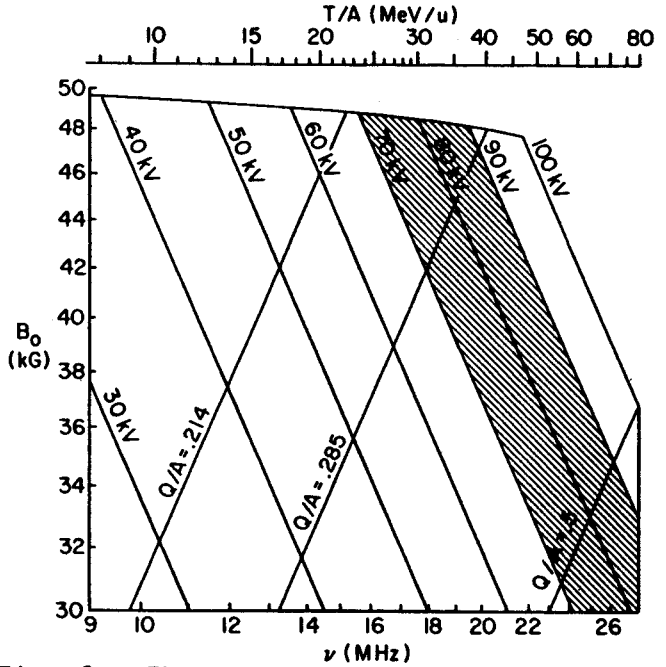

Fig. 3. The operating diagram of the K500 cyclotron using the pig source is shown. The ECR operating diagram must be increased 8% above these value, because of differences in the central region. The shaded area in the region now possible for experiments due to corona improvement. The charge to mass ratios at the shaded area limits also indicate the beams effected. Additional studies are now needed to determine the limitations above 90 kV.

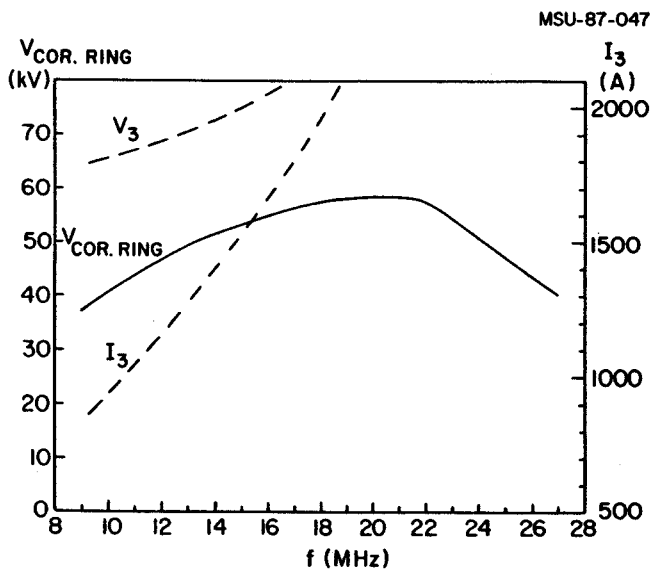

Fig. 4. The corona ring voltage versus frequency is shown and peaks at 58kV. The cyclotron is normally operated in a constant geometry mode, hence requiring less voltage at low frequency. The distance of the corona ring from the shorting plane, hence its voltage, becomes less for the high frequency mode. The combination of conditions peaks between 17 and 22 MHz. This voltage must be maintained across the directly coupled plastic cooling lines. I_3 in the current at the corona ring. V_3 is the dee voltage to produce 58kV at the corona ring.

withstand the rf voltage applied to the electrode during operation. In the rf amplifiers the maximum voltage is 20 kV peak; on the dee stem corona ring it is 60 kV peak. Figure 4 shows the expected voltage on the corona ring as a function of frequency where the cyclotron is operating in the fixed orbit mode having approximately 500 turns.

The water lines are made to spiral around the stem, making a complete 360° circle before coming in contact with the corona rings. The water lines enter the resonator through ports formerly used for neutralizing loops, and they do not restrict the travel of the shorting planes. Initially only one plastic water line was inserted and found that it could successfully withstand voltage breakdown over the expected operating range. Next a plastic cooling line with a transition to a short copper metal part that was temporarily attached to the dee stem at the corona ring location was tested. Then a set of corona rings with an embedded water line was constructed and installed (see Figure 5). Finally, all the corona rings were modified to have direct water cooling.

The operating experience with direct water cooling on all corona rings for several months has been as follows. Thermal measurements of the corona ring surface indicates that these rings are operating very cool. Figure 6 is the

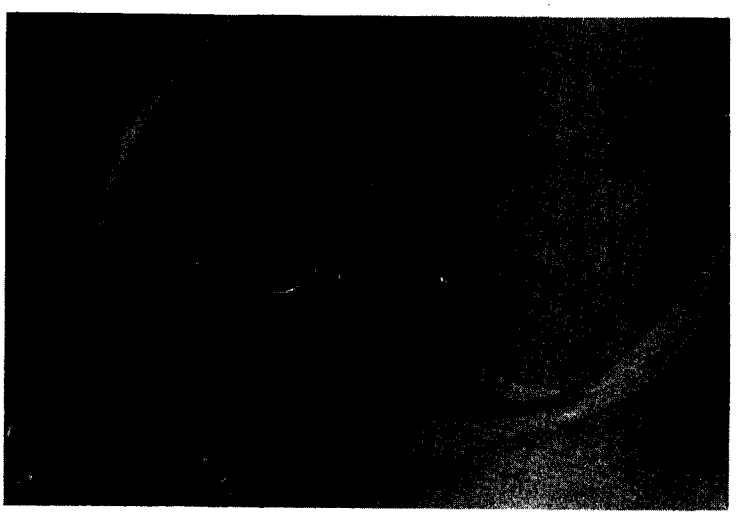

Fig. 5. A photograph of an installed water cooled corona ring. The plastic hose spiral 360° from input to contact with the corona ring in crossing the rf gap.

thermal history of the B corona rings, where U is the upper and L is the lower ring. The temperatures from the measurements have been normalized to the temperature expected at 27.5 MHz and 100kV, namely the rf maximum power operating point. The first data point is the temperature before the corona ring modification where it was found that the lower ring could get as hot as 500° F. The other points are for the corona rings after the modification and indicate a temperature of about 150° F.

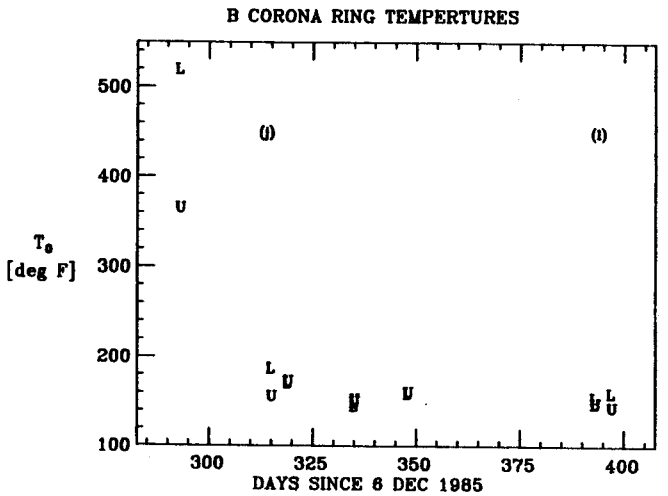

Fig. 6. Thermal history of the B corona rings is shown. The temperature data is normalized to 27.5MHz and 100kV. The first data points are for the uncooled corona rings and indicates they would operate at 500° F at maximum rf power. The cooled rings appear to operate at about 150° F.

The next important result is the successful operation of the rf system at 85 kV. The expanded operating range of the cyclotron can be seen in Fig. 3. For example, 60MeV/u deuterons (Q/A = .5) have been run. The dee voltage has been operated at 90 kV, although the dees were sparking but appeared to be baking in after about four hours. Deflector sparking may also be a limitation on the maximum beam energy.

The plastic water lines have developed several leaks at the fittings, but they were quickly detected and the fittings tightened. In summary, the direct water cooled corona rings appear to be an acceptable fix.

Acknowledgement: The contribution of the following people to the successful construction and installation of the water cooled corona rings is greatly appreciated. A. McCartney, S. Hickson, D. Navarre, G. Humenik, G. Horner, M. Garbek, and A. Thulin.

References

1. NSCL Annual Report (1985) 119.
2. NSCL Annual Report (1983-84) 205.

MAGNET SUPPLY INSTALLATION AND CONTROL FOR THE ECR ION SOURCE COMPLEX

W. Nurnberger, T. Antaya, L. Foth, and J. Vincent

During its development period and first year of operation, the Room Temperature ECR ion source (RT-ECR) used trim coil power supplies from the K-800 cyclotron project to supply power for its magnet coils and for the various magnets in the beam line leading from the RT-ECR to the K-500 cyclotron. These supplies were controlled by spare K-500 trim coil supply controllers, which were in turn controlled by a VME/Fermi system located in the temporary ECR control console, via an 'octal' serial communication system.

With the K-800 cyclotron project progressing toward completion, it became necessary to make a transition to dedicated power supplies for the ion source and associated K-500 beam line magnets. In addition, planning for the operation of a second ECR and possibly a third, as well as for the installation of a beam transport line to the K-800 cyclotron, made it clear that a centralized control area for the ion sources and cyclotron injection beam lines would be the most efficient way to implement controls for all of these systems.

With these objectives in mind, a plan for upgrading the ECR complex was made. The power supplies and various other equipment had been ordered and were beginning to arrive, so that when a time slot in the K-500 operations schedule opened up in mid-December, 1986, the implementation plan and the major equipment was ready.

This report describes the resulting control system from a power supply control viewpoint. Enough general information is included to provide an overview of the total ion source control system.

Equipment Layout

The ECR complex is located in the West high bay between the K-500 and the K-800 cyclotrons. It includes the Room Temperature ECR ion source, the DC magnet and high voltage bias supplies, the microwave power supplies, and the ECR control console. This equipment is grouped in a relatively compact arrangement. There is room in this area for the Compact ECR ion source (C-ECR), presently under construction; and for the Superconducting ECR ion source (SC-ECR).

The magnet supplies and their controls are located in three sets of equipment racks: a 5 bay unit, a 3 bay unit, and in a single bay unit composed of two large supplies placed one above the other. Equipment in these racks is generally grouped according to the major unit it serves.

In the 5 bay unit, 2 bays are for equipment associated with the RT-ECR, 1 bay is for K-500 beam line equipment, and 1 bay is for C-ECR equipment. The remaining bay houses the VME/Fermi control system for both the equipment in the other 4 bays of this unit, and for the C-ECR and K-500 beam line equipment located in the 3 bay unit. It also contains the Modicon 884 PLC used to provide interlocking and on-off control functions for the equipment in both the 5 bay and 3 bay units.

In the 3 bay unit, 1 bay is reserved for SC-ECR equipment and the VME/Fermi system for controlling the SC-ECR and the K-800 beam line equipment. The second bay holds K-800 beam line equipment, and the third bay holds C-ECR and K-500 beam line equipment.

Control Signal Path for a Typical Controlled Device

The ECR magnet supplies are controlled by a VME/Fermi system located in the equipment racks containing the supplies. This VME/Fermi system communicates with the VME/Fermi system in the ECR control console (and eventually with the main control system) through the ARC Net serial system. Thus, the Fermi console at the ECR control console can be used to set and read values in the supply control system.

The VME/Fermi system that controls the magnet supplies resides in a VME card cage that also contains several standard VME A/D and D/A cards. These are connected to the VME/Fermi system via the VME bus on the backplane of the card cage. This arrangement allows the VME/Fermi system to generate analog command signals to control the supplies, and to read the various analog monitor signals from the supplies.

Following the analog command signal from the D/A card as an example (see Fig. 1), the output of the VME D/A card is connected to a terminal strip in a cable breakout box, located in the upper rear of one of the equipment racks, by a twisted pair, shielded ribbon cable. The breakout box serves several functions. First, since the D/A card's output connector contains more than one output signal, it provides a way of splitting up these command signals into separate cables, one for each supply. Second, by arranging the contents of each breakout box to include terminal strips connected to A/D cards as well as D/A cards, a single cable carrying both the command and monitor signals can be run to each supply in an efficient and orderly manner. Third, the open terminals in the breakout box provide a centralized point where signals may be measured for trouble-shooting. Fourth, the breakout box provides a place to sort out the various signal ground connections and arrange them to eliminate

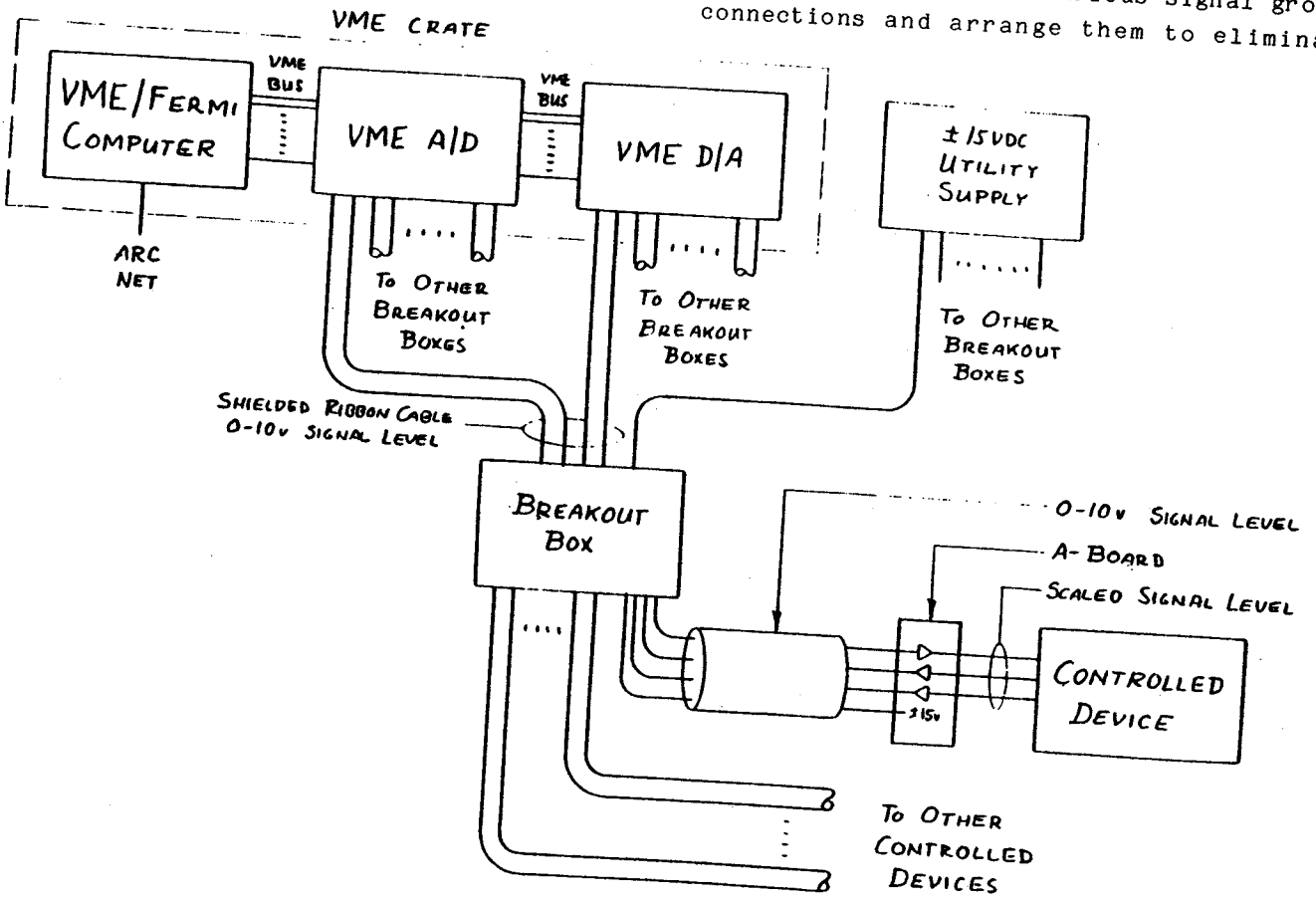

Fig. 1. Signal flow block diagram for a single device.

grounding problems. Finally, it provides a place to insert various utilities, such as power for the signal conditioning board, in the cables running to the supplies.

The command signal, combined with several other signals in an individually shielded, multiple twisted pair cable, now goes to a signal conditioning board (an 'A-board'), normally located on the back of the controlled supply. The A-board also has several functions. First, it scales the D/A card output level (0 - 10 volts for the cards generating the magnet supply command signals) to levels which are compatible with the command signal input requirements of the individual supply. This scaled command signal is then applied through a short jumper to the command input terminals of the magnet power supply. Second, the A-board similarly scales the monitor signals from the magnet supply to the VME A/D card's full scale range of 0 - 10 volts. Third, the scaling amplifiers on the A-board are designed so that, by adding a few parts in places already allocated on the board, they can be used as low pass filters if this function is required to reduce the noise level on the command and/or monitor signals. Finally, they also incorporate metal oxide varistor (MOV) devices to protect themselves and the rest of the control system from high voltage transients.

It should be noted that controlling magnet supplies is only one task of the ECR's VME/Fermi system. It also controls the various HV bias supplies associated with ECR operation and injection of the beam into the cyclotron, and it controls the amplitude of the RF voltage on the beam buncher electrodes. In addition to these control functions, the VME/Fermi system also monitors various instruments associated with the operation of the ECR ion source system so they can be read by the ECR console VME/Fermi station or by any other station on the ARC Net system. For example, A-boards convert the outputs of vacuum gauges to signal levels compatible with the VME A/D cards. B-boards convert beam currents at various points in the beam transport system to voltages which can also be read by the VME A/D cards. There are approximately 120 analog input points and 40 analog output points serviced by the present system. See Fig. 2 for the signal flow diagram for the entire system.

Technical Details

Control Voltages -

Because the VME/Fermi control equipment is placed near the equipment it controls and monitors, -10 to +10 volt or 0 - 10 volt DC signals can be used to transport control information to and from the various devices without excessive noise problems. These particular ranges were selected because they are full scale ranges for commercially available VME A/D and D/A modules.

Grounding -

Since the ECR complex resides in one compact earth ground environment, it was not necessary to electrically isolate the controlled devices from the controller at either end of the control signal lines. This allowed the use of non-isolated VME A/D and D/A modules, which are relatively inexpensive.

However, this lack of isolation does place rather stringent restrictions on the location of allowable grounds in the system. For example, if a magnet's winding or either of its lead wires is grounded at any point (say, to provide transient protection), control of that magnet's supply is lost. To provide the protection mentioned in the example, MOV devices are connected from each magnet terminal to ground. In addition, a resistor is placed across the magnet coil to provide a load to dissipate any energy induced in the coil by sparking or other transients. Experience has shown that this protection is necessary because an arc from the ECR vessel, which is biased at a high voltage, to ground tends to induce EMF in the magnet coils.

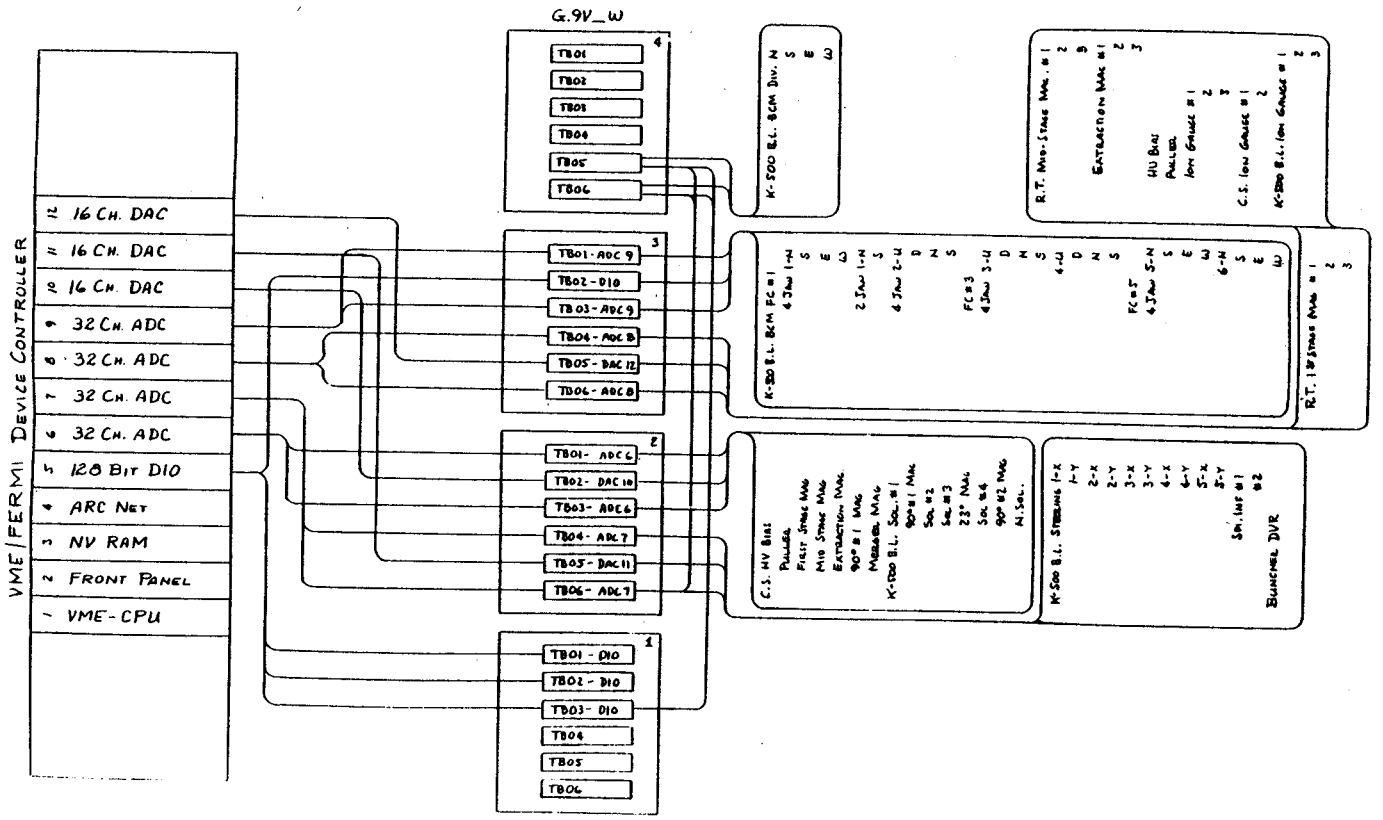

Fig. 2. VME system signal flow diagram.

The 'A' Board -

In the ECR complex, the most common controlled device is a power supply. Each power supply has a command input (for example, current set), and two monitor outputs (for example, load current and voltage). As mentioned above, these signals are processed by an A-board which is normally mounted in, on, or near the controlled device.

The A-board is a small (approximately 1" x 6") printed circuit board which interfaces to the world through a screw terminal strip mounted along one side. It was designed specifically to interface the magnet power supplies to the VME control system, since there are more magnet supplies than any other single type of device. Thus, it has three data channels: One is intended to receive the 0 - 10 volt current set signal from the VME D/A and reduce it to the 0 - 100 mV current set signal required by the supply. The other two are intended to take the load voltage (0 - V) and load current (0 - 100mV) signals from the supply and scale them to the 0 - 10 volt full scale signals required by the VME A/D. However, the A-board was designed to be versatile enough to easily accommodate other devices by simply changing a few component values to adjust scaling factors, or by leaving

some part of the board un-populated if fewer channels of data are required. The A-board receives its operating power from a central ±15 volt power supply and thus does not depend on the equipment it services for power. Approximate cost for an A-board is $39.

The B-board -

Although not a part of the magnet power supply control system, the B-board is described here for completeness. The B-board circuit is a dual range transconductance amplifier designed specifically to convert the beam current at various points in the ECR beam transport system (0 - 10 μa or 0 - 1000 μa) to the 0 - 10 volt signal level used for the VME/Fermi system's A/D inputs. The B-board circuit board is housed in a small metal box which may be located near the measuring point to reduce the length of the low level cable. The ±15 volt utility supplies power to the board along the same cable that carries the output signal to and the range command signal from the VME/Fermi system. Approximate cost for a B-board is $40.

Operating Experience

The ECR VME/Fermi control system was installed during a cyclotron shutdown which ran from December 10, 1986 to January 10, 1987. The RT-ECR was running on January 8. In this same period, several other major portions of the ECR complex were also rearranged and upgraded: the entire control console was rebuilt, expanded, and moved to a new location; the AC power system to run the new magnet supplies was installed; cable trays to support the magnet leads were installed; new magnet leads were run; etc. In spite of all this happening in one small area, the work was well enough organized so that surprisingly few errors were made and the RT-ECR was up and running within a day or two of applying power to the systems.

At the time of writing, the magnet supply control system has been in operation about two months. Other than a few initial problems with inadvertent grounds, operation has been trouble-free. Even sparking between various parts of the RT-ECR and ground, which caused considerable difficulty with the old system, has caused no trouble since the installation of the new system.

LOW ENERGY BUNCHER FOR THE K500 CYCLOTRON

F. Marti, J. Moskalik and J. Vincent

The low energy beam line considered here is the line transporting the ECR beam into the K500 cyclotron. In the last portion of this line the beam is injected through an axial hole in the yoke.

The buncher is placed at z=-1.7 m below the median plane. It is a single gap buncher of a design similar to the Argonne low energy buncher.[1] Two molybdenum grids, 4 cm in diameter, 0.0127 cm thick with a distance of 0.152 cm between wires, are placed 0.7 cm apart.

The grids are mounted in two cones that expand away from the grids (see Figure 1). The purpose of the cones is to increase the distance over which the voltage change from ground to RF voltage is applied, and thus minimize the effect of the fringe field. Orbit tracking in the buncher electric field has shown this geometry to be effective. Figure 2 shows the equipotentials in the electrostatic field calculated with POISSON. Figure 3 shows the effect of the fringe field on the longitudinal component of the ion velocity. The grids are placed at z= 300 mm in the calculation. Two different ions with an RF phase difference of 180° are plotted. As we can see, the velocity change produced by the fringe field is negligible.

One of the two grids is excited with the first harmonic of the RF voltage while the

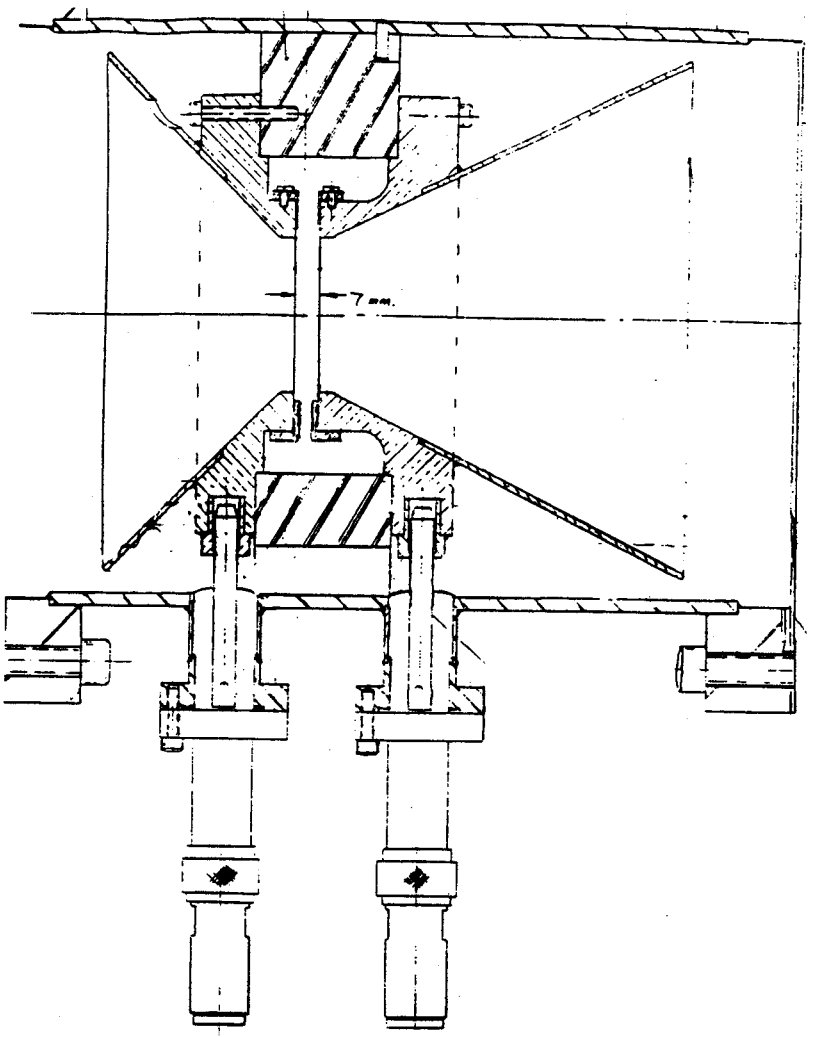

Fig. 1 Cross section of the buncher showing the grids mounted on the conical electrodes.

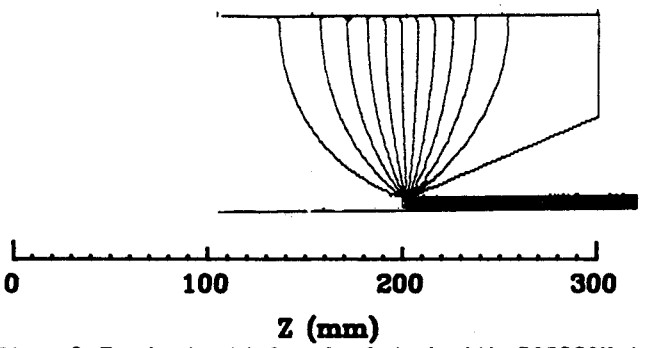

Fig. 2 Equipotential calculated with POISSON in the fringe field region.

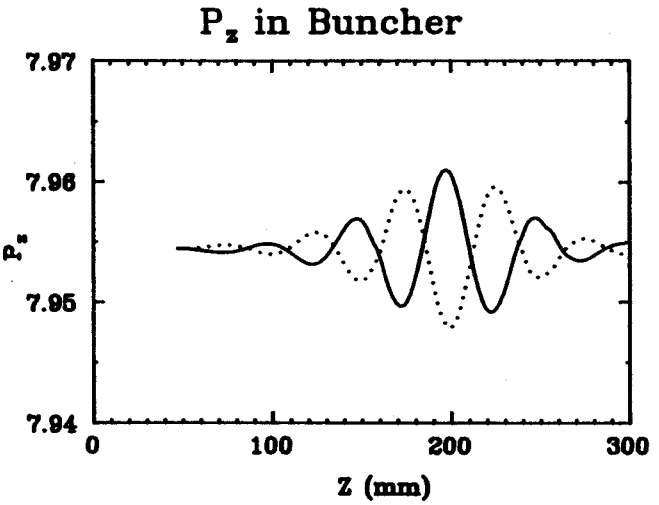

Fig. 3 Momentum along the axis in the fringe field region for two ions that are 180 RF degrees out of phase.

second remains grounded, or is excited with the second harmonic.

As we showed in Ref. 2, the yoke traversal and inflector contribute greatly to the time spread of the beam at the median plane. To estimate the effect of this debunching we simulated a beam with a circular phase space in (x,x') given by:

$$x^2 + x'^2 \leq 100 \ , \quad x \text{ in mm and } x' \text{ in mrad} \quad (1)$$

and a current density given by:

$$I = e^{-d^2} \ , \text{ where } d^2 = (x^2+x'^2)/100. \quad (2)$$

These ions were tracked through the axial yoke and spiral inflector and their arrival time at the median plane calculated.

The buncher efficiency, defined as the current captured in a ± 20° phase range divided by the 360° current, is shown in Fig. 4.

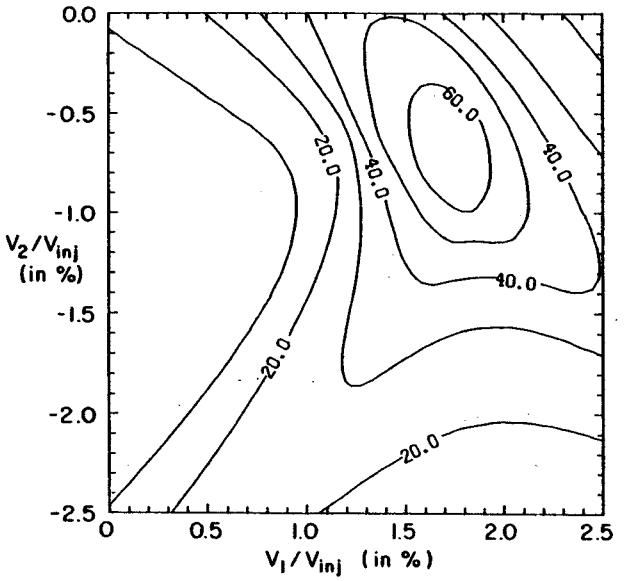

Fig. 4 Buncher efficiency (current in a ±20° interval divided by the 360° current) as a function of the first and second harmonic voltages. The time spread introduced by the yoke and inflector has been convoluted with the buncher time change. A circular beam in (x,x') space with a gaussian profile has been assumed (see text).

RF design

The bunching structure consists of two conical electrodes, each with a grid, spaced 7 mm apart (refer to figure 1). Since the size of this structure with respect to the operating wavelengths is small, the structure may be modeled as a pie arrangement of lumped capacitors. The measured values of these capacities are listed on figure 5 as the buncher electrode equivalent circuit. Currently the second harmonic grid is grounded to allow proper operation when excited only at the fundamental frequency.

The basic electrical model is a small capacitive load (buncher electrodes), connected to a short flexible coaxial section, connected to a large variable capacitive shunt, connected to a shorted rigid coaxial section. The flexible section was used so that the structure

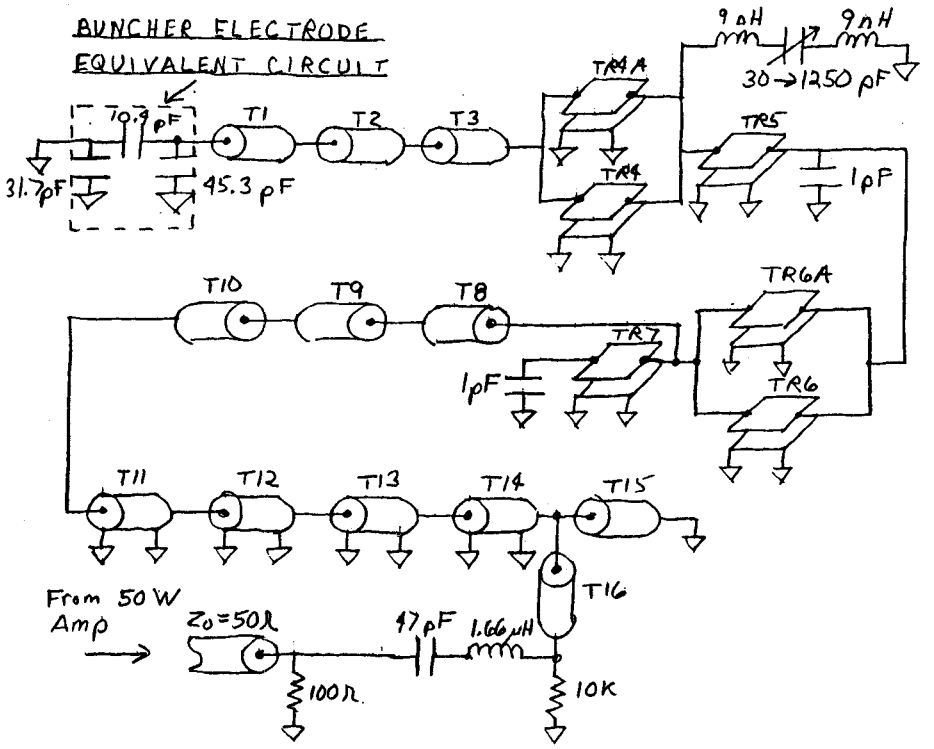

Fig. 5. Beam buncher schematic diagram.

could be easily installed or moved. The rigid structure also contains the magnetic coupling loop and a variable vacuum capacitor used to tune the resonator. Although many transmission lines and lumped elements are necessary to accurately model the structure, most of these are a consequence of the mechanical design rather than as a result of any electrical requirements.

Since the resonator structure is basically an inductive stub,(less than 45 degrees long to make things easy) capacitively tuned at the loaded end to achieve resonance, and the power linearly decreases with increasing frequency; coupling is possible broadband. This allows the loop coupling to be adjusted during initial setup and left fixed forever after. The impedance looking into the coupling port varies from 40 to about 80 Ohms throughout the frequency band of 9 to 27 Mhz. Therefore, the only tuning required is achieved by adjusting the variable capacitor in a well defined fashion. The structure requires about 20 Watts to maintain 500 Volts peak on the buncher grid at 9 Mhz, and about 8 Watts at 27 Mhz for the same conditions. The buncher is entirely tuned and operated remotely. Tuning is accomplished from the K500 rf balcony, and buncher voltage and phase may be adjusted from either the rf balcony or the main control room.

This was the first structure designed using the newly developed RF algorithm called "RESON". The structure behaved exactly as predicted and was installed and placed in operation almost immediately after initial assembly. The system has operated trouble free since the initial installation. Figure 6 is a block diagram of the entire buncher system.

A mirror image of this block diagram with minor additions would be required to bring the second harmonic on line. The increased bunching efficiency (which would result if the second harmonic is activated) may not be worth the increased cost, and the manpower to accomplish this goal is not available at this time due to the K800 design and construction demands.

We would like to thank Dr. R. Pardo for sending us detailed information on the Argonne buncher.

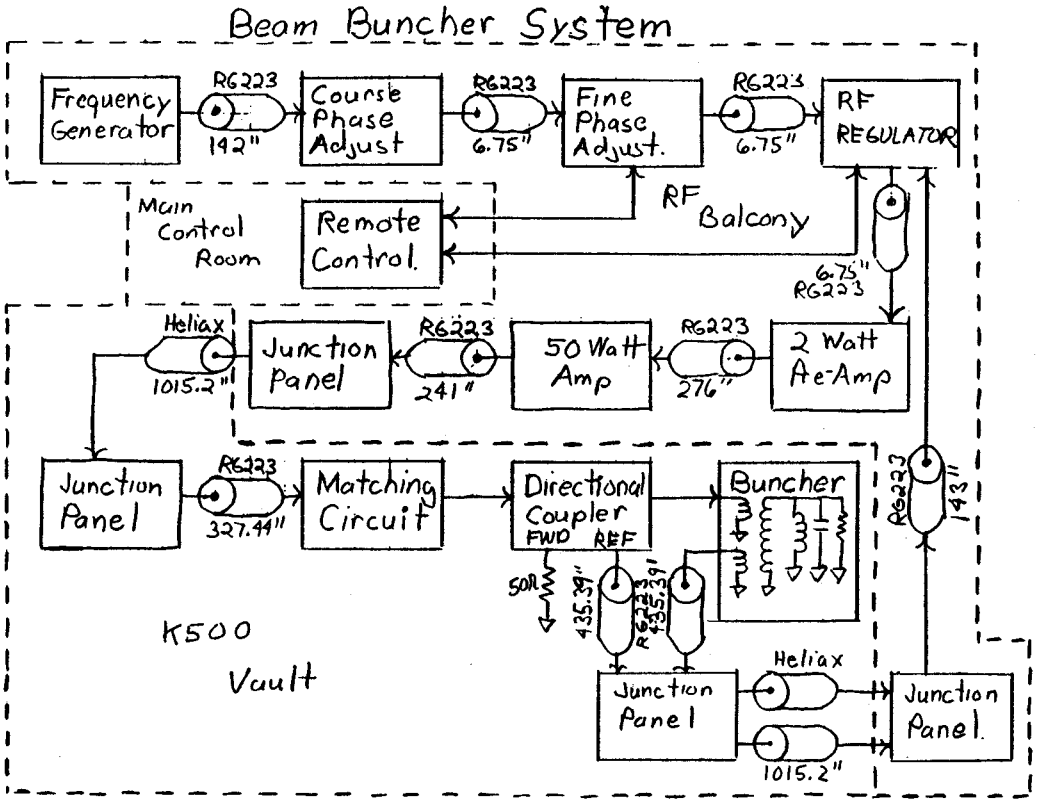

Fig. 6. Beam buncher block diagram.

References

1. F. J. Lynch et al., Nucl. Inst. and Methods 159, 245 (1979). R. Pardo, personal communication (1985).
2. F. Marti et al., IEEE Trans. Nucl. Sc. NS-32, 2450 (1985).

EXPERIMENTAL FACILITIES OPERATION

R. Blue, N. Anantaraman, R. Ronningen, and J. Winfield

During the period covered by this report several experiments were run which required special target chambers rather than the laboratory's "standard" experimental facilities. These experiments were run at either the Users Station in the south vault or the Neutron Station in the north vault. The measurements of gamma-ray circular polarization were made at the Users Station, but limits on available space and accessibility at that location have tended to favor the Neutron Station for larger setups. Measurements of high-energy gamma rays by the Stevenson group, measurements of the production of high energy light particles by Becchetti et al., neutron measurements by Galonsky et al., and a particle-gamma correlation experiment by an NSCL/University of Pittsburgh collaboration were run at the Neutron Station. The apparatus for the latter experiment included four of an eventual six Ge detectors equipped with BGO Compton suppression shields and a 14 element BGO multiplicity detection array from the Pittsburgh/MSU multidetector array. Although resources for the development of additional facilities have been limited by the demands of the K-800 construction schedule, as the above examples indicate, we have been able to accommodate experiments with special needs.

Improvements to the facilities include the installation of a 2000 liter per second turbo pump on the 60-inch chamber as a replacement for the cryopump previously in use there. With this pump it is possible to pump down from atmosphere without use of the Roots blower system. The primary reason for this change was that the cryopump tended to warm up when counter gases leaking into the chamber became a significant part of the gas load.

Some progress has been made toward improving the resolution of both the RPMS and the S-320 spectrometers. For the RPMS the improved resolution is achieved by moving the focal plane further from the last quadrupole doublet. A new support structure is under construction to provide a convenient means for positioning detectors at the new focal plane position. Also new power supplies, capable of providing higher currents for the last quadrupole doublet, are being installed. Investigations of the resolution of the S-320 have clarified the requirements for proper tuning of the beam line, but some improvement in the position resolution of the focal plane detector will be needed before the resolution limit of the magnetic elements can be achieved.

Except for the new pump installation for the 60-inch chamber, we continue to rely on cryopumps for most of the beam line and experimental chambers. On average these pumps seem to require extensive cold-head maintenance about once a year. Several of the helium compressors have been in service for more than 35,000 hours. We have been advised by the manufacturer that compressor failure can be expected after as few as 20,000 hours. With that in mind we may soon begin to experience an upturn in the number of compressor failures even though that has not been our experience to date. The small (150 liter/second) turbo pumps used as portable pumping systems throughout the laboratory continue to give reliable service.

Power supplies for the magnetic elements of the beam transport system and their controls remain major sources of problems. The multi-output Perkin supply that powers most of the beam line quadrupole magnets is particularly

failure prone. We continue to replace the banks of pass transistors with a new design using silicon transistors as the old banks of germanium transistors fail. So far none of the new banks has failed. Of particular concern now are failures in the current regulation and control circuits. Many of these failures involve an on-card voltage regulator that is obsolete. When we exhaust our remaining small stock of these regulators we will have to work out a modification of the current shunt amplifiers in order to keep this supply operating.

During this operating period we have seen a significant increase in the variety of beams accelerated by the K-500 cyclotron, both with regard to energy range and masses. The ECR ion source has permitted the development of many new beams while the upgrade of some parts of the RF system and operation in the second harmonic mode have extended the range in operating energy upward and downward, respectively. Generally these changes have been accommodated by the beam transport system without difficulty, but there does remain the longstanding problem that the sensitivity of the devices used for beam detection sets a lower limit on the beam intensity required for tuning the beam transport system.

NUCLEAR ELECTRONICS DEVELOPMENT

M.R. Maier, M. Robertson, James Vincent

As we have said in last years report, the task of the Electronics group can be divided into two parts: one part is the development of modules for "small" experiments (less than 50 detector channels) and the other part is the development of modules for "large" experiments (more than 100 detector channels). "Small" electronics come normally in NIM modules; "large" come in CAMAC.

At this time, in addition to the 4X4 logic and the quad gate generator, we have finished the construction of 20 quad "fast slow" amplifier modules, and 20 quad fast amplifier modules. All four of these modules are shown in the photograph to demonstrate the high density of connections and controls of the front panels. The quad "fast slow" amplifiers contain four slow shaping amplifiers 1μs to 7μs and four fast "timing filter" amplifiers.

The gain of the slow channels can be varied with a coarse switch and a ten turn fine gain helipot from less than 10 to more than 1000. Peaking times of 1,3,5 and 7μs, unipolar or bipolar, can be selected with switches inside the module. The gain of the fast channels can be changed from 3 to 1000, and differentiation and integration time constants between 10ns and 300ns can be selected with switches inside the module. Output amplitudes are +8V into 1KΩ on the slow channel, with a 50Ω series termination resistor, and -4V into 50Ω on the fast channel (rise time < 20ns). The quad fast amplifier contains four amplifier channels with a fixed gain of 8. They have three separate outputs; the output amplitude is +200mV to -3V on 50Ω, and the rise time is less than 1ns. They are AC - coupled with a time constant of 5μs. These modules have been used by MSU staff in experiments at GANIL and at Berkeley.

In addition, we have built five channel charge preamplifiers for use with position sensitive propositional counters and photo-multiplier divider strings for use in vacuo.

The high density CAMAC modules for the 4π detector are not finished yet. Closest to completion is the Octal CAMAC Constant Fraction Discriminator, whose production has been contracted to industry.

The requirements in the near future seem to point in the direction of building large numbers of "low cost" devices, e.g. preamps, shaping amplifiers, and specialized electronics, e.g. pulse shape discriminators.

Since we now have a Computer Aided Design Station (CAD), we intend to pursue more ambitious projects like ECL - trigger modules for the 4π array and perhaps even a modern peak-sensing ADC.

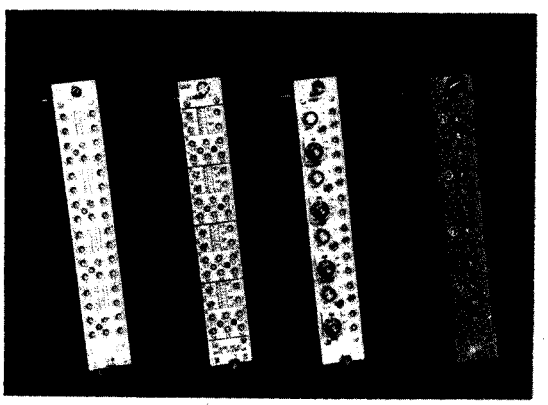

Fig. 1 Four NIM modules designed in house from left to right: 4X4 logic, quad gate generator, quad fast-slow amplifier, and quad fast amplifier. Note the high density of LEMO connections-"swiss cheese front panel"-on the first two modules.

N. Anantaraman and E. Kales[a]

"NUCLEAR PHYSICS PREPRINTS", an on-line database and monthly newsletter, has been in existence for five years. The project was started in recognition of the fact that preprints are a vital communication medium among scientists in fast-developing fields. Its major aim is to provide timely flow of information in the nuclear physics community through the dissemination of pertinent facts on preprints received at the NSCL. This has been achieved by mailing out monthly newsletters to about 500 nuclear subscriber-contributors around the world and on-line through TELENET and FTS.

Most recently, the project was supported by a grant from the U.S. Department of Energy, Office of Scientific and Technical Information, to Professor Peter Signell of the Department of Physics and Astronomy, Michigan State University. But the grant was discontinued effective September 1, 1986, and the NSCL has taken over the project for a few months, until a decision is reached on how and whether the project should be funded in the long run. We believe that it serves a valuable function in the nuclear physics community. This belief is based on a survey conducted in the summer of 1985 among the community of users on their perceptions of the system. The results of the survey were strongly positive. We have applied to the National Science Foundation for funds to continue the project.

We are in the process of transferring the data storage function from the central computer at the University of Michigan to the Vax-780 computer at the NSCL. This should make the on-line database feature of the system easier to use. We are investigating whether it is worthwhile to continue this on-line feature. In the past, it took a disproportionate amount of effort and was seldom used by the community.

We solicit preprints from nuclear scientists who are not already on our mailing list. All one has to do to join us and receive the newsletter is to notify us and send a copy of each preprint produced by one's group to the compilation address.

N. Anantaraman, Librarian
National Superconducting Cyclotron Laboratory
Michigan State University
East Lansing, MI 48824-1321
U.S.A.

---

a. Department of Physics and Astronomy, Michigan State University